Atmospheric Environment 79 (2013) 7–19

Contents lists available at SciVerse ScienceDirect

Atmospheric Environment

journal homepage: www.elsevier.com/locate/atmosenv

Aerosol properties and radiative forcing over Kanpur during severe aerosol loading conditions

D.G. Kaskaoutis [a], P.R. Sinha [b], V. Vinoj [c], P.G. Kosmopoulos [d], S.N. Tripathi [e], Amit Misra [e], M. Sharma [f], R.P. Singh [g,*]

[a] Department of Physics, School of Natural Science, Shiv Nadar University, Dadri 203207, India
[b] National Balloon Facility, Tata Institute of Fundamental Research, ECIL Post 5, Hyderabad 500 062, India
[c] Pacific Northwest National Laboratory, Richland, WA 99352, USA
[d] Laboratory of Meteorology, Department of Physics, University of Athens, Athens, Greece
[e] Department of Civil Engineering, Indian Institute of Technology, Kanpur, India
[f] Research and Technology Development Centre, Sharda University, Greater Noida NCR 201306, India
[g] School of Earth and Environmental Sciences, Schmid College of Science and Technology, Chapman University, Orange, CA 92866, USA

HIGHLIGHTS

- Studying the seasonal and inter-annual variation of the aerosol episodes (AE) over Kanpur, central IGP, India.
- The AE days are associated with accumulation of anthropogenic aerosols and biomass burning during post-monsoon and winter.
- The AE days are strongly related to dust presence during pre-monsoon and monsoon.
- The optical and physical properties of aerosols significantly are modifying during the AE days, also depending on season.
- The aerosol radiative forcing at surface, TOA and within the atmosphere is considered very high during the AE days.

ARTICLE INFO

Article history:
Received 1 March 2013
Received in revised form
6 June 2013
Accepted 10 June 2013

Keywords:
Severe aerosol
Optical properties
Radiative forcing
Kanpur AERONET

ABSTRACT

The present work analyzes the aerosol episode (AE) days and examines the modification in aerosol properties and radiative forcing during the period 2001–2010 based on Kanpur-AERONET data. AEs are defined as the days having daily-mean aerosol optical depth (AOD) above the decadal mean + 1 STD (standard deviation); the threshold value is defined at 0.93. The analysis identifies 277 out of 2095 days (13.2%) of AEs over Kanpur, which are most frequently observed during post-monsoon (78 cases, 18.6%) and monsoon (76, 14.7%) seasons due to biomass-burning episodes and dust influence, respectively. On the other hand, the AEs during winter and pre-monsoon are lesser in both absolute and percentage values (65, 12.5% and 58, 9.1%, respectively). The modification in aerosol properties on the AE days is strongly dependent on season; during post-monsoon and winter, the AEs are associated with enhanced presence of fine-mode aerosols from anthropogenic emissions and/or biomass burning, while during pre-monsoon and monsoon seasons, they are mostly associated with dust. Aerosol radiative forcing (ARF) calculated using SBDART shows much more surface (~−69 to −97 Wm^{-2}) and Top of Atmosphere cooling (−20 to −30 Wm^{-2}) as well as atmospheric heating (~43 to 71 Wm^{-2}) during the AE days as compared to seasonal means. These forcing values are mainly controlled by the higher AODs and the modified aerosol characteristics (Angstrom Exponent α, single scattering albedo SSA) during the AE days in each season. Furthermore, the vertical profiles of aerosols and atmospheric radiative heating exhibit significant increase in lower and mid troposphere during the AE days. This may cause serious climate implications over Ganges Basin and surrounding regions with further consequences on cloud microphysics, monsoon rainfall and melting of Himalayan glaciers.

1. Introduction

Aerosols over south Asia have attracted the global scientific interest due to severe loading, especially over northern India and

* Corresponding author.
E-mail address: rsingh@chapman.edu (R.P. Singh).

1352-2310/$ – see front matter © 2013 Elsevier Ltd. All rights reserved.
http://dx.doi.org/10.1016/j.atmosenv.2013.06.020

Indo-Gangetic Plains (IGP), that constitutes a major environmental and climatic issue (Goloub et al., 2001; Menon et al., 2002; Ramanathan et al., 2005; Dey and Tripathi, 2007, 2008; Gautam et al., 2010). Aerosols over IGP exhibit a pronounced seasonal and interannual variability (Kaskaoutis et al., 2011) strongly dependent on anthropogenic and natural aerosol emissions, local and regional meteorology and atmospheric dynamics (Reddy and Venkataraman, 2002; Nair et al., 2007; Abish and Mohanakumar, 2011). During winter season, the whole IGP region is under the influence of frequent foggy and hazy conditions that are source of several problems e.g., being inimical to human health, deterioration of air quality, poor visibility, delaying or even canceling of flights and road accidents (Gautam et al., 2007; Das et al., 2008; Badarinath et al., 2009a, 2011). Earlier studies (Srivastava et al., 2012a; Misra et al., 2012) have shown a thick aerosol layer near the surface composed of a large anthropogenic fraction during winter, while in late pre-monsoon and early monsoon (April–June), dust presence at higher altitudes increases the aerosol load in the vertical, since the area is strongly affected by frequent and intense dust storms originating from Thar desert and/or Arabian Peninsula and Middle East (e.g. El-Askary et al., 2006; Prasad and Singh, 2007a; Gautam et al., 2009a; Guleria et al., 2011). The period mid-June to September is the rainy season over IGP; the aerosol loading is reduced due to rain washout (Dey and di Girolamo, 2010), while significant variability in aerosol loading at different temporal scales is observed due to changes in onset, intensity and duration of monsoon (Gautam et al., 2009b; Bhawar and Devara, 2010; Manoj et al., 2011). Post-monsoon season is well known for the crop residue burning over northwestern IGP (Sharma et al., 2010; Mishra and Shibata, 2012). These agriculture activities lead to a dense-smoke environment and under favorable conditions smoke plumes may cover the whole IGP or even affecting central-south India (Badarinath et al., 2009b) and Arabian Sea (Badarinath et al., 2009c).

The seasonally-changed meteorological patterns, air mass trajectories and boundary layer dynamics are the main factors for different atmospheric conditions and aerosol types over IGP. In general, the aerosol optical depth (AOD) is higher during May–June due to mixing of desert dust and anthropogenic aerosols (Singh et al., 2004; Dey et al., 2005), while high AODs are also observed during winter due to increased biomass burning and bio-fuel combustions (Streets et al., 2003; Venkataraman et al., 2006; Lu et al., 2011). Long-term satellite observations from MODIS and MISR have shown that during winter season, high AOD regions swing over the eastern IGP depending upon the weather conditions, while in May–June the AOD gradient is westward shifting (Prasad and Singh, 2007b; Kaskaoutis et al., 2011).

Therefore, studying the severe aerosol episodes (AEs) over northern India has a significant importance in the climatic, atmospheric and human health points of view. These episodes lead to high-AODs on specific days throughout the year, when the aerosol loading and aerosol radiative forcing (ARF) are much higher than the mean levels (Singh et al., 2010). Days with severe aerosol and pollution conditions may be related to enhanced anthropogenic emissions as on the days of Diwali festival (Barman et al., 2008), intense dust outflows (Dey et al., 2004), increased biomass and agriculture burning (Krishna Prasad et al., 2012), absence of precipitation and longer aerosol lifetime (Ghude et al., 2011), temperature inversions and lower mixing height (Srivastava et al., 2012a). Depending on local meteorological conditions, the periods of persistent high AOD over the region may be about 5–10 days, able to affect the atmospheric heating rate (Tripathi et al., 2007; Jaidevi et al., 2011; Srivastava et al., 2012b) as well as human health (Jaidevi et al., 2009), since in the vast majority of the cases the locally-emitted aerosols and pollutants are of fine size and easily inhalable.

The present study focuses on analyzing the seasonality of the AEs detected over Kanpur AERONET site (26.5°N, 80.2°E), located in central IGP. Days with daily-mean AOD_{500} above the decadal (2001–2010) mean + 1STD (standard deviation) are considered as AEs, on which the aerosol characteristics (AOD, Angstrom exponent, columnar size distribution) are examined vis-a-vis the decadal means. Such a comparison allows us to understand the reasons and define the additional aerosol loading causing the episodes in the different seasons. Furthermore, the ARF at surface, top of atmosphere (TOA) and within the atmosphere is examined for the seasonal means and on the AE days in order to understand the climatic response of the severe aerosol-laden atmospheres over IGP. The present work is the first of its kind performed over Kanpur examining the seasonal variation and the specific aerosol characteristics on days with extreme AOD values.

2. Data and methodology

Due to global scientific interest in aerosol properties and their climate implications in northern India, the first AERONET station equipped with the Cimel (CE-318) sun/sky radiometer was established at IIT Kanpur campus in 2001 (Singh et al., 2004). The Cimel gives the spectral AOD at eight wavelengths (340–1640 nm), Angstrom exponent α (440–870 nm) and the water vapor content (WVC) at 940 nm using its internal calibration for direct-beam irradiance recordings (Holben et al., 1998). Furthermore, the Spectral Deconvolution Algorithm (SDA) retrieves the aerosol columnar size distribution (CSD), single scattering albedo (SSA) and asymmetry parameter (g) from the almucantar measurements performed at large (above 50°) solar zenith angles and $AOD_{440} > 0.4$ (Dubovik et al., 2000). The sun photometer recordings are performed for clear skies, with limited observations during the rainy season. The Level 2 (cloud screened and quality assured) AERONET data over Kanpur were used in the present work, considering the uncertainties in the retrievals described elsewhere (Dubovik et al., 2000; Smirnov et al., 2000). Furthermore, Ångström exponent (α) values defined at shorter (380–500 nm) and longer (675–870 nm) wavelengths were also analyzed on the AE days and compared with the seasonal mean (2001–2010) values. All the aerosol properties are daily averaged and analyzed on monthly and seasonal basis during the period January 2001 to December 2010. From the whole data series (2095 daily AOD_{500} values) a mean AOD_{500} of 0.63 ± 0.30 was found. The AEs over Kanpur are defined as the days with daily mean AOD_{500} above the critical threshold $\overline{AOD}$ + 1STD = 0.93.

In addition to the study of aerosol optical and physical properties, shortwave (0.3–4.0 μm) ARF calculations at surface, TOA and within the atmosphere were also performed for two groups of data (seasonal means and seasonal-averaged AEs) by combined use of Optical Properties of Aerosols and Clouds (OPAC) (Hess et al., 1998) and Santa Barbara Discrete ordinate Atmospheric Radiative Transfer (SBDART) (Ricchiazzi et al., 1998) models. In order to perform ARF calculations in the shortwave spectrum, aerosol properties in the entire wavelength region (0.3–4.0 μm) are necessary. Since the measured AERONET aerosol optical properties are not available beyond 1.64 μm, we run the OPAC model and reconstructed the measured aerosol parameters (SSA, g) by varying the aerosol components (water soluble, insoluble, sea salt, dust) that contribute to the aerosol properties. The output parameters in OPAC are the AOD, α, SSA, g; the WVC was obtained from AERONET and columnar ozone from TOMS and OMI satellite sensors, separately for the seasonal means and the AE-means for each season. The measured BC mass concentration at Kanpur was used as input

for the soot component (number concentration) in OPAC, and the number concentrations for the other aerosol types, i.e. water soluble, insoluble, sea salt and dust were adjusted iteratively until the OPAC derived spectral AODs were consistent with the AERONET retrievals (root mean square error lower than 0.03), and the AERONET and OPAC-simulated values of α, SSA and g were similar (Das and Jayaraman, 2011; Sinha et al., 2013a). In this way, new aerosol mixtures have been defined from OPAC simulations to best fit the observations and to derive the required optical properties, vis spectral distribution of AOD, SSA, g and α values. An average relative humidity (RH) value (measurements from Kanpur meteorological station) was calculated in each season for the seasonal means and AEs. It should be noted that higher RH values were associated with intense foggy conditions in winter and dust storms in late pre-monsoon/monsoon compared to the respective seasonal means. The closest OPAC-fixed RH value to the means for each group was used in the computations, since aerosol properties vary as a function of RH (Ramachandran and Kedia, 2012).

The radiative transfer code SBDART is based on the discrete ordinate (DISORT) approach for a vertically inhomogeneous, non-isothermal, plane-parallel atmosphere, and is known for its reliability and computational efficiency in solving the radiative transfer equations. The surface albedo is an important parameter for the radiative transfer calculations, since elevated absorbing aerosols above highly-reflecting surfaces can heat more the lower atmosphere and change the sign of forcing from cooling to heating (Satheesh et al., 2010). The 8-day Terra-MODIS (Global 500m) surface reflectance values over Kanpur at seven wavelengths from visible to IR (0.469, 0.555, 0.645, 0.859, 1.24, 1.64 and 2.13 μm) have been used as input in SBDART to model the spectral shortwave (0.3–4.0 μm) surface reflectance using a combination of water, sand and vegetation (Pathak et al., 2010; Ramachandran and Kedia, 2011). The combination of vegetation, sand and water has been done in appropriate proportions such that the resultant spectrum matches the MODIS-derived surface reflectance. The ARF values were integrated for the whole day in each season and AEs. The atmospheric heating rate due to aerosol forcing is calculated following Liou (2002):

$$\frac{\partial T}{\partial t} = \frac{g}{C_p}\frac{\Delta F}{\Delta P} \quad (1)$$

where $\partial T/\partial t$ is the heating rate (K day^{-1}), g is the acceleration due to gravity, C_p the specific heat capacity of the air, ΔF the resultant atmospheric forcing and ΔP the atmospheric pressure difference between surface and 3 km, considered to be 300 hPa. The atmospheric heating rates were also calculated over Kanpur in each season, for the decadal mean, and for the AE days.

3. Results and discussions

3.1. Identification of the aerosol episodes

Fig. 1 shows the daily variation of AOD_{500} over Kanpur during the period Jan 2001–Dec 2010. The mean AOD_{500} value of 0.63 is drawn (red bold line) along with the mean + 1STD (0.93) line (dotted), while an increasing trend of 7.69% was found during the measurement period (Kaskaoutis et al., 2012a). From the whole dataset, 277 cases (13.2%) were found to exceed the threshold value corresponding to AE days, exhibiting significant seasonal and yearly variability depending on atmospheric and meteorological conditions, anthropogenic and natural aerosol emissions. The analysis shows that 65 AEs out of 519 daily AOD observations (12.5%) occurred in winter (Dec–Feb), while during pre-monsoon (Mar–May), monsoon (Jun–Sep) and post-monsoon (Oct–Nov) seasons, the corresponding numbers are 58 (9.1%), 76 (14.7%) and 78 (18.6%), respectively.

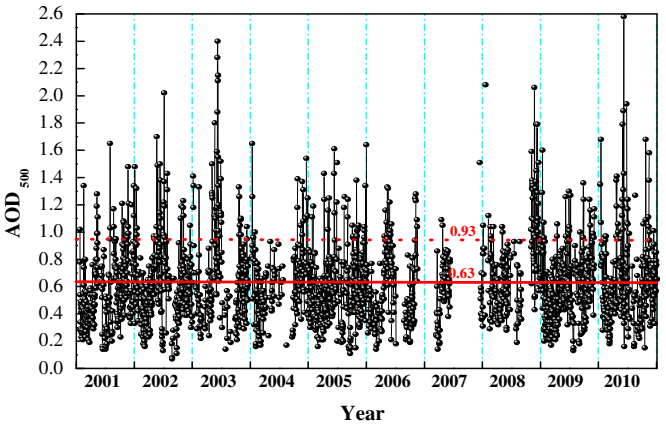

Fig. 1. Daily variation of the AOD_{500} at Kanpur AERONET station during the period January 2001 to December 2010. The mean value (in bold red) and the upper threshold (mean + stdev) for the identification of the aerosol episodes are also given. (For interpretation of the references to color in this figure legend, the reader is referred to the web version of this article.)

Table 1 summarizes the results about the frequency of AEs over Kanpur in absolute and percent (%) values, revealing a considerable seasonal and interannual variation. However, it should be noted that due to the presence of clouds and calibration protocol, aerosol observations are not equally distributed within the months and years, and a large gap of data from December 2006 to February 2007, and from June 2007 to November 2007 exists. The main finding from Table 1 is the large number (20 out of 31 cases, 64.5%) of AEs in post-monsoon 2008 as well as during the monsoon seasons of 2002 and 2003 and pre-monsoon of 2003. Several AEs also occurred during winter 2008 with 16 peaks out of 44 daily AOD observations (36.4%).

The frequency of occurrence of the AE days is further examined on monthly basis along with the monthly-mean AOD_{500} variation (Fig. 2) revealing a co-variance between the two parameters. Therefore, the highest frequency of AE days is observed during May–June and November–January, which are the months with the highest AOD_{500}. In absolute terms, November exhibits the highest number (56) of AEs, whereas the % percentages are similar for June and November. In contrast, the lowest monthly AOD_{500} is seen in March, which exhibits only one AE.

The AEs over Kanpur occur either on specific days or periods of 2–5 consecutive days (Fig. 3) under favorable atmospheric and meteorological conditions, i.e. surface or height inversions during winter trapping the pollutants near the ground, enhanced subsidence, absence or deficit of rainy washout, increased biomass and bio-fuel combustion mainly during winter cold nights and persistent transport of dust plumes from the west (Prasad and Singh, 2007a; Eck et al., 2010). The AEs usually last one day at the vast majority of the cases; however, AEs are also persistent over Kanpur for about a week (4–6 consecutive days). The most extreme cases are the duration of AEs for 11 days during the period 4–14 June 2003 and for 12 days during the period 3–14 November 2008. Table 2 summarizes the AOD_{500} and Angstrom exponent (α) values for the AE days in each season. The AOD_{500} means are in the range of ~1.15–~1.29, while the seasons (pre-monsoon/monsoon and post-monsoon/winter) clearly differentiate based on α (much higher values for the latters).

3.2. Changes in Angstrom exponent

This section examines the changes in Angstrom exponent values on the AE days as compared to the seasonal means, which are

Table 1
Number and percentage (in brackets) of aerosol-episode days over Kanpur for each season and year during the period 2001–2010.

	2001	2002	2003	2004	2005	2006	2007	2008	2009	2010
Winter	6 (9.52)	5 (7.57)	6 (12.77)	8 (14.29)	7 (9.33)	0 (0)	1 (10)	16 (36.36)	9 (15.79)	7 (10.14)
Pre-monsoon	5 (7.14)	6 (8.57)	10 (22.73)	0 (0)	5 (5.95)	12 (21.43)	2 (3.92)	3 (4.54)	2 (2.29)	13 (19.12)
Monsoon	8 (10.67)	14 (17.95)	18 (41.86)	0 (0)	10 (13.69)	1 (3.12)	0 (0)	2 (6.67)	12 (12.63)	11 (16.67)
Post-monsoon	10 (19.23)	5 (9.80)	7 (12.28)	7 (16.29)	9 (15.25)	6 (19.35)	0 (0)	20 (64.51)	5 (10)	9 (20)
Whole	29 (11.15)	30 (11.32)	41 (21.46)	15 (9.32)	31 (10.65)	19 (12.58)	3 (4.41)	41 (23.98)	28 (9.69)	40 (16.13)

strongly influenced by enhanced local emission or intense aerosol plumes transported from long distances. Fig. 4 shows the distribution of the α values for each season in box and whiskers charts view. More specifically, the α values are examined in three spectral bands, i) 440–870 nm (the standard wavelength region for AERONET retrievals), ii) 380–500 nm and, iii) 675–870 nm. The boxes in Fig. 4 correspond to 50% of the values distribution (from 25% to 75%), while the square and line within the boxes indicate the mean and median values, respectively. The x and – symbols correspond to 1%/99% and min/max values, respectively.

The results show that the four seasons can be divided in two groups, i) post-monsoon/winter and, ii) pre-monsoon/monsoon. The main difference between the two groups is the spreading of α values, which is lower during post-monsoon and winter seasons compared to the rest of the year. This indicates well-defined aerosol sources concerning the particle size in winter and post-monsoon, and multiplicity of sources in the rest of the year, as also shown by Singh et al. (2004) and Eck et al. (2010). Besides this, a significant finding is the different behavior of α values on the AE days. Thus, the $\alpha_{440-870}$ and $\alpha_{675-870}$ values increase during post-monsoon and winter, suggesting enhanced presence of fine-mode aerosols and fine-to-coarse mode ratio (Reid et al., 1999), respectively. Thus, it is indicated that the severe AODs during post-monsoon and winter seasons are associated with increasing emissions of anthropogenic aerosols either from industries, coal thermal power plants, automobile exhausts, bio-fuel combustions and biomass burning of the crop residue (Prasad et al., 2006; Kirpa et al., 2010, 2012; Singh, 2010; Prasad et al., 2012; Kaul et al., 2011). These urban/anthropogenic aerosols are highly hygroscopic in nature and serve as the condensation nuclei for the formation of fog and hazy conditions during winter, favored by the lower temperatures decreasing the super-saturation point (Ganguly et al., 2006; Patidar et al., 2012). In contrast, during pre-monsoon and monsoon, the α values at all wavelengths decrease significantly during the AE cases indicating dominance of coarse-mode aerosols and increase in coarse-mode fraction. This suggests that the sources for the high-AOD further from the local background are natural in origin corresponding to dust plumes transported from the west or re-suspension of mineral dust in the urban environment during prolonged dry periods (Srivastava et al., 2012c). Srivastava et al. (2012d) found dominance of polluted dust aerosol type over Kanpur during pre-monsoon, while the carbonaceous aerosols (mostly BC and organic carbon) contributed only a few to the total AOD.

On the other hand, the $\alpha_{380-500}$ values seem to have decreased in all seasons during the AE cases compared to the seasonal means. According to Reid et al. (1999) this suggests increase in fine mode particle size corresponding to coagulation process that is much more favored under turbid atmospheres. This was also shown by Gobbi et al. (2007) and Wang et al. (2011) using a specific identification scheme for examining the aerosol modification processes over Kanpur via the relationship of α and dα. More specifically, both studies revealed a shift toward higher fine-mode radius for increasing AOD during winter season. Further, Eck et al. (2012) emphasized on the bimodality in the submicron range of the aerosol size distribution caused by coagulation and/or hydration processes during foggy/cloudy days. Recently, Kaskaoutis et al. (2012a) showed a shift in the submicron size distribution toward larger radius during the period 2006–2010 compared to 2001–2005 under a more turbid environment (statistically significant increase in AOD during November–December). This suggests that the increased emissions of fine-mode aerosols over IGP are able to produce a second aerosol generation of larger submicron size.

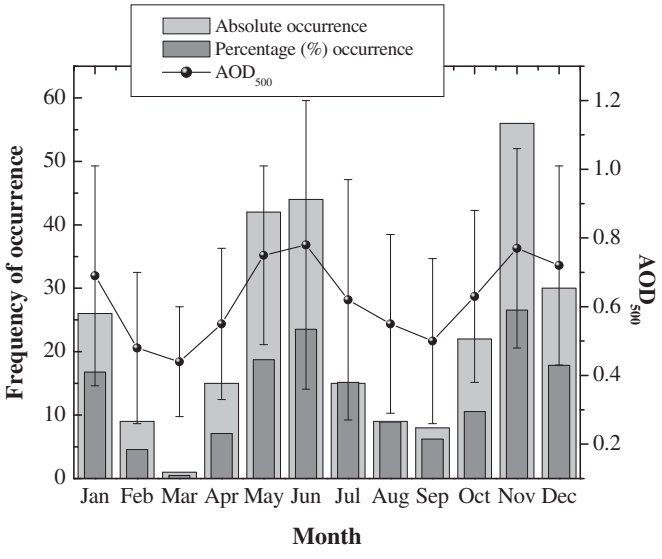

Fig. 2. Monthly variation of the absolute and percentage (%) occurrences of the aerosol-episode days along with the monthly mean AOD_{500} over Kanpur during the period 2001–2010.

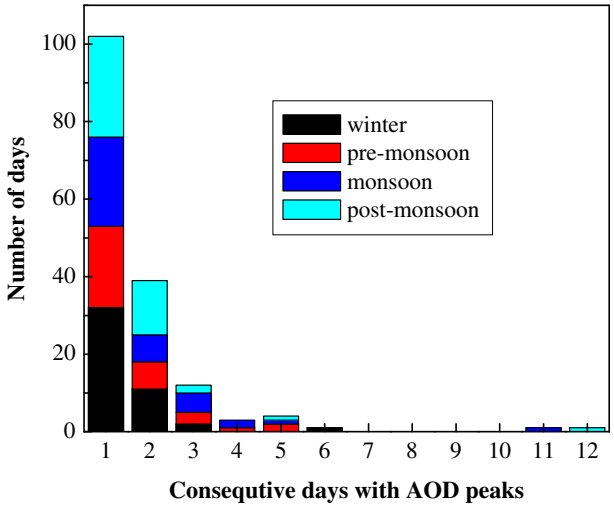

Fig. 3. Seasonal variation of the consecutive aerosol-episode days at Kanpur AERONET station.

Table 2
Seasonal mean aerosol optical properties on the aerosol-episode days over Kanpur during the period 2001–2010.

	AOD	α (440–870)	α (380–500)	α (675–870)
Winter	1.20 ± 0.26	1.20 ± 0.21	0.76 ± 0.16	1.42 ± 0.25
Pre-monsoon	1.15 ± 0.21	0.32 ± 0.35	0.37 ± 0.35	0.30 ± 0.33
Monsoon	1.29 ± 0.37	0.36 ± 0.41	0.36 ± 0.33	0.37 ± 0.42
Post-monsoon	1.16 ± 0.20	1.30 ± 0.11	0.86 ± 0.131	1.52 ± 0.14

3.3. Modification in columnar size distribution (CSD)

The aerosol optical properties strongly depend on the columnar size distribution (CSD) that determines the scatter of incident solar radiation, while Eck et al. (2005, 2010, 2012), Kaskaoutis et al. (2012a,b) and Sinha et al. (2012) have shown that the CSD is closely related to α, derivative of Angstrom exponent (α'), fine-mode fraction and their variations. Thus, the particle size and fine-to-coarse mode ratio are interesting to be examined during the AEs over Kanpur and for further understanding of the modification of the CSD from the seasonal mean. Fig. 5 shows the seasonal means of CSDs for the period 2001–2010 and for the AE days. The number of available almucantar retrievals for obtaining the seasonal means (see figure caption) is considered satisfactory, while the uncertainties in the retrievals are about 15%; however, the available CSDs are much lesser in number than the α values (Fig. 4.) Nevertheless, in all seasons the modification in CSDs on AEs is closely related to the changes in α (Fig. 4). More specifically, during winter and post-monsoon seasons, the CSD on AEs shows a pronounced increase in fine-mode fraction, which is consistent with the statistically significant increase in $\alpha_{675-870}$. This increase is more intense during the winter season, while the higher CSDs for the AEs are attributed to the more turbid atmospheres. Furthermore, an increase in fine-mode radius is clearly shown in Fig. 5a, d, which reflects decrease in $\alpha_{380-500}$ (Fig. 4a, d) during the AEs. As discussed above, such findings suggest coagulation of the fine mode under severe turbid atmospheres and indicate that aerosols over IGP during winter are classified as urban/industrial type with significant influence of biomass burning either from fossil fuel or bio-fuel combustion (Kar et al., 2010; Verma et al., 2012). In contrast, no significant change is found in the coarse-mode radius. The results in Fig. 4b, c showed a decrease in $\alpha_{380-500}$ on the AE days during pre-monsoon and monsoon. A near absence of fine-mode with concurrent shift toward coarse-mode is shown in the respective CSDs (Fig. 5b, c). The coarse mode in CSD during pre-monsoon and monsoon is ~3 times larger than the seasonal mean indicating that the additional AOD is composed by coarse-mode aerosols, i.e. dust transported via long distances, or emitted and re-suspended locally.

3.4. Modification in α vs $d\alpha$ plot

The wavelength dependence of AOD as well as the curvature of lnAOD vs lnλ is closely associated with aerosol CSD (Eck et al., 1999, 2005, 2010; Schuster et al., 2006). The above-mentioned studies have shown different wavelength dependence of α based on the

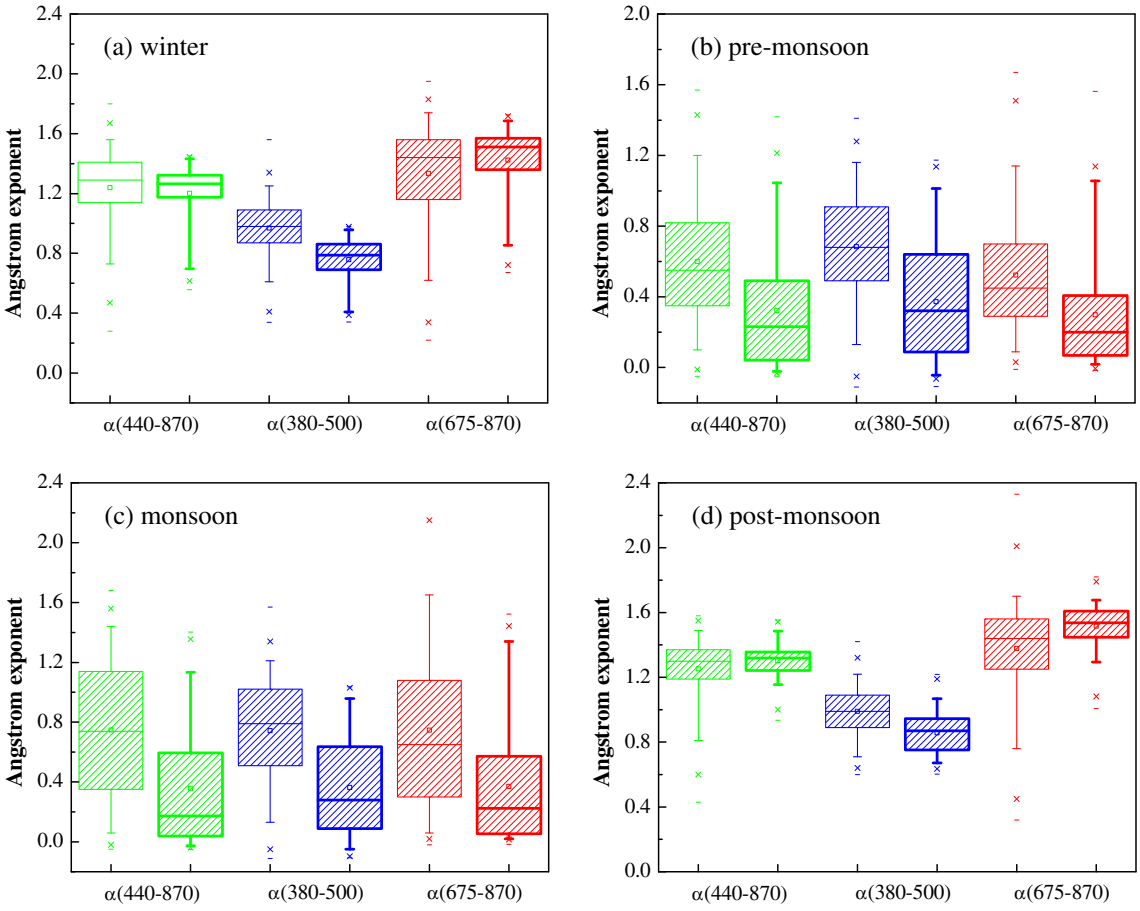

Fig. 4. Seasonal box charts of Angstrom exponent values for different spectral bands at Kanpur AERONET station for the period 2001–2010 and for the aerosol-episode days (bold borders). The statistical significant differences of the mean values between the two groups are defined by the filled boxes.

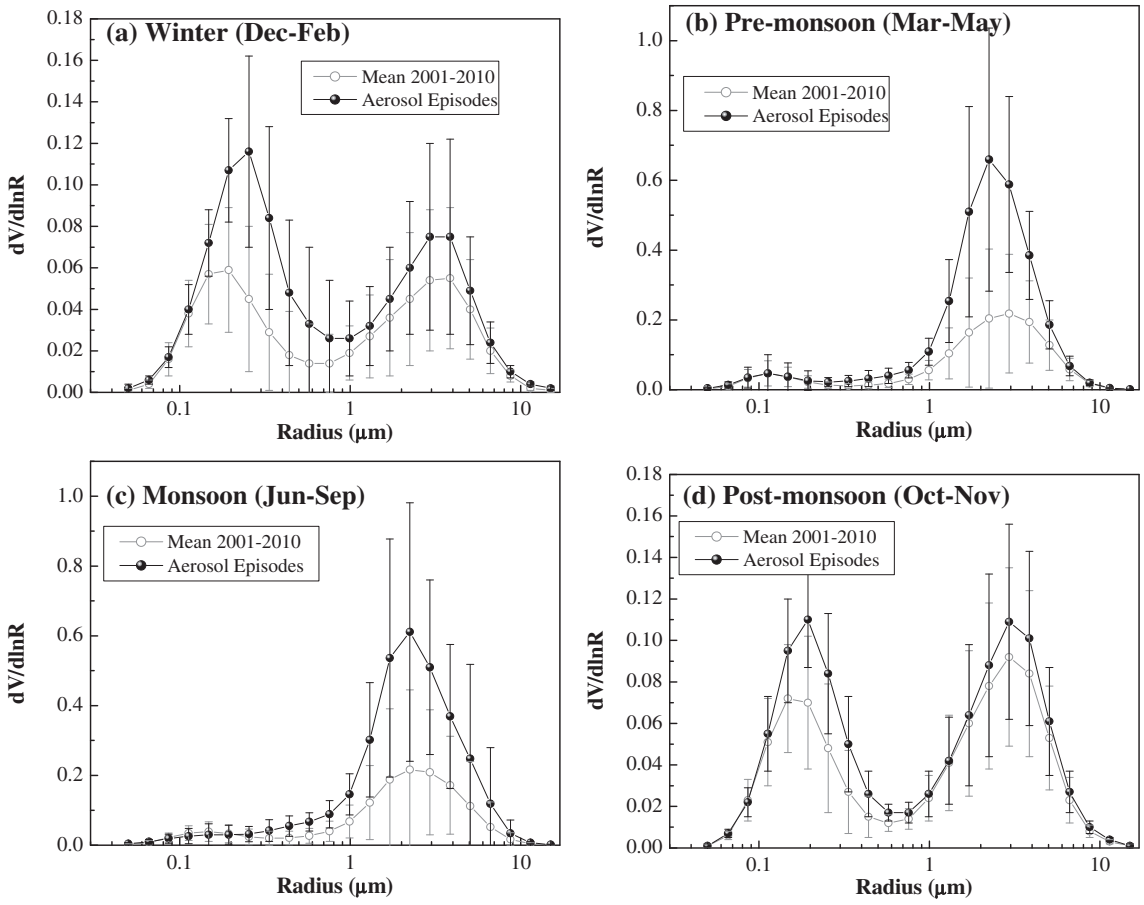

Fig. 5. Seasonal mean columnar size distributions at Kanpur AERONET station for the period 2001–2010 and for the aerosol-episode days. The vertical bars correspond to one standard deviation from the mean. The number of available CSDs for the period 2001–2010 and for the aerosol-episode days is: 312, 32 for winter, 353, 27 for pre-monsoon, 185, 25 for monsoon and 225, 46 for post-monsoon.

aerosol particle size and coarse-to-fine mode ratio. Furthermore, Figs. 4 and 5 reveal that the seasonally-changed atmospheric conditions prevailing during the AE days influence the α values as well as the CSDs.

Fig. 6 applies the aerosol identification scheme, first proposed by Gobbi et al. (2007), in order to further examine the modifications in several aerosol properties, such as fine-mode radii, fine-mode fraction, Angstrom exponent, etc during the AE days for each season. This scheme combines α and its spectral variation dα ($\alpha_{440-675}-\alpha_{675-870}$) with the radius of fine-mode particles (R_f) and the fine-mode fraction (η) as the grid parameters in grouped AOD. The scheme has been extensively used for aerosol type identification at several AERONET sites (Gobbi et al., 2007; Basart et al., 2009; Yoon et al., 2011) as well as in Kanpur (Wang et al., 2011). In the present case, the AERONET retrievals are classified in two groups for each season: a) the whole dataset in the period 2001–2010 and, b) the AEs focusing on the changes in α vs dα pattern between the two groups. The results show that during post-monsoon and winter, the AEs are associated with more negative dα values and slightly lower $\alpha_{440-870}$ than the decadal means. The AEs in these seasons are associated with high η (>70%) and, as the AOD increases the R_f shifts toward higher values. These findings suggest additional fine-mode aerosol loading on the AE days and evidence of aerosol coagulation under severe turbid atmospheres. On the other hand, in pre-monsoon and monsoon, the vast majority of the cases exhibit positive dα, thus highlighting the coarse-mode dominance associated with low η (<50%). The AEs in these seasons exhibit a shift toward the origin (α, dα = 0) along a nearly constant R_f of ~0.12–0.15 μm and continuously decreasing values of η. These findings suggest negligible variation in fine-mode radii and a significant increase in coarse-mode fraction; these conditions are characteristic of enhanced dust contribution at higher AODs (Kaskaoutis et al., 2012b). The results obtained from the identification scheme are in absolute agreement with those found from CSDs and the variations in spectral α, thus highlighting the

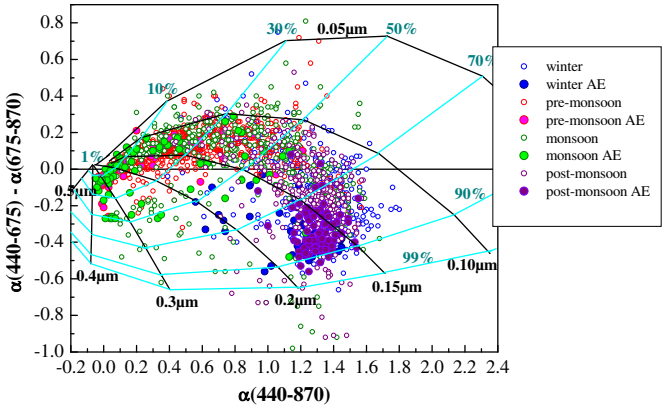

Fig. 6. Correlation of α (440–870) with dα ($\alpha_{440-675}-\alpha_{675-870}$) values over Kanpur for each season and separately for the AE days.

significance of its application for monitoring the modification of aerosol properties under changing atmospheres.

The current results reveal different aerosol optical, physical properties and types depending on season over central IGP. Mishra and Shibata (2012) have classified the aerosol types (dust, biomass burning and urban pollution) over Kanpur by examining the absorbing Angstrom exponent (AAE) and extinction Angstrom exponent (EAE) values along with CSD based on 5-year (2006–2010) AERONET data. More specifically, they reported enhanced presence of dust aerosols during the pre-monsoon and monsoon seasons, dominance of urban/industrial pollution during winter season and enhanced biomass burning along with urban pollution during post-monsoon. Similarly, Giles et al. (2011) grouped the aerosols over Kanpur in three categories in the framework of TIGERZ experiment, viz. i) mostly dust, ii) mixed BC and dust and, iii) mostly BC using AAE, EAE, fine-mode fraction and sphericity fraction.

3.5. Aerosol radiative forcing

Using the methodology described in section 2, OPAC and SBDART models were jointly utilized to calculate ARF over Kanpur both for seasonal means (2001–2010) and for the season-averaged AEs. The OPAC-estimated spectral AODs are, in general, close to the measured ones (Fig. 7) and within the standard error of the measurements (rms error <0.03) suggesting that the procedure adopted for the estimation of aerosol mixing and ARF is quite robust. In this respect, α values from OPAC are close to those of AERONET at both shorter and longer wavelengths. However, the inconsistency seems to be higher for the AE days, especially during pre-monsoon. On the other hand, the AERONET retrievals of SSA and g via SDA depend on several assumptions (particle sphericity) that may cause some discrepancy in the absolute values (Dubovik and King, 2000). Nevertheless, OPAC-simulated and AERONET SSA exhibit a satisfactory agreement (not shown) and similar spectral pattern, i.e. increasing trend with wavelength during pre-monsoon/monsoon and decreasing in post-monsoon/winter. It was found that OPAC estimates lower SSA values compared to AERONET, with differences lying in the range of 0.55% (for monsoon seasonal mean) to 10.4% (for winter AEs), on spectral average.

Fig. 8 exhibits the volume mixing ratio (%) of the different components that are used for the aerosol mixture in OPAC. Accurate estimate of the aerosol mixing state is essential for an accurate assessment of ARF, since rough assumptions can lead to large uncertainties in aerosol climatic effects. In the current analysis, the external mixing state of aerosols is considered. In addition to the external mixing, recent studies over Kanpur (Dey et al., 2008; Srivastava and Ramachandran, 2013) have shown that core-shell mixing is also a probable scenario, in which BC and dust play a crucial role during post-monsoon/winter and pre-monsoon/monsoon seasons, respectively. The water-soluble aerosol component, mainly consisting of anthropogenic aerosols (i.e. ammonium, nitrate, chloride and sulfate), is the dominant type with contribution of ~50–65% during winter and post-monsoon (for both cases),

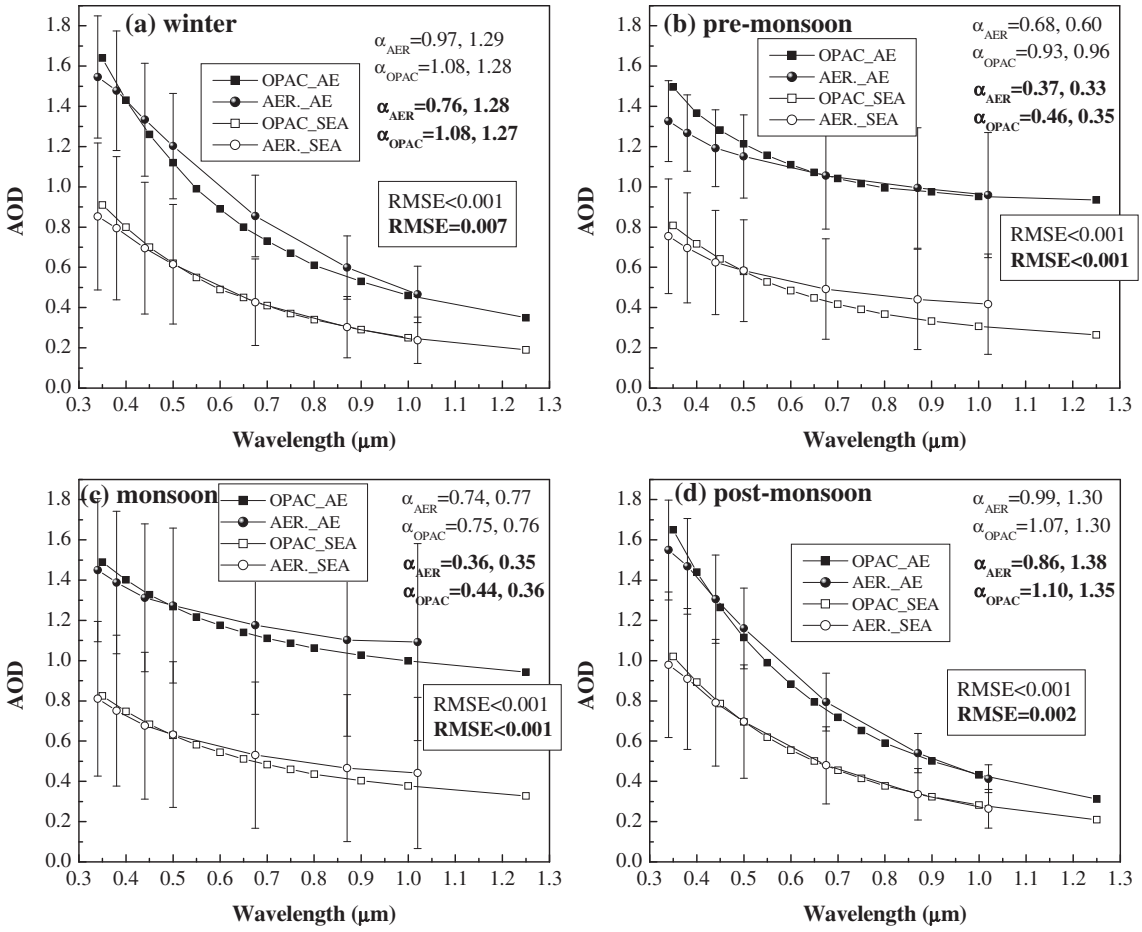

Fig. 7. Spectral AOD variation as obtained from AERONET measurements and OPAC simulations for seasonal and AE means. The vertical bars correspond to one standard deviation from the seasonal mean. The root mean square error (RMSE) corresponds to AOD_{500} values (bold for AEs), while α is defined at shorter (380–500 for AERONET and 350–500 for OPAC) and longer (500–870 for AERONET and 500–800 for OPAC) wavelengths (after commas) for both seasonal means and AEs (bold).

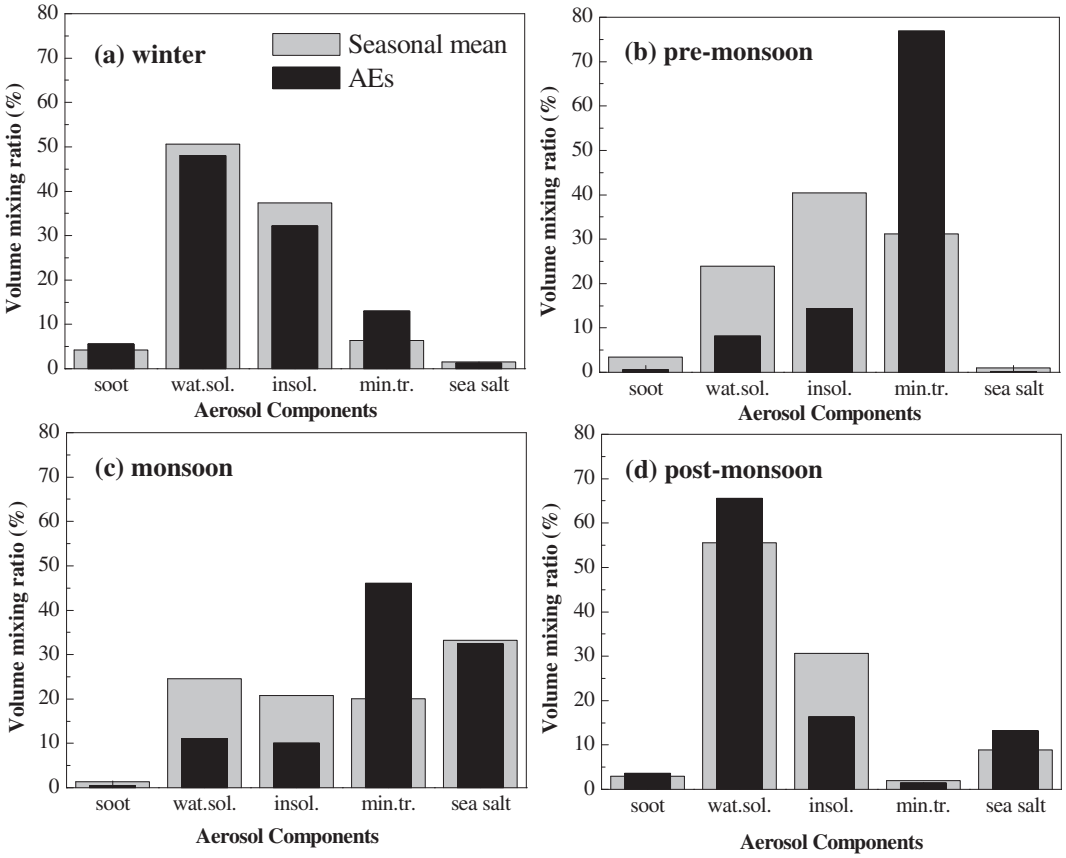

Fig. 8. Volume mixing ratios (%) of various aerosol components as obtained from OPAC simulations for the seasonal means and the AEs.

while it is lower during pre-monsoon and monsoon (<25%). The insoluble aerosols (soil and fly ash, organics) present lower contribution in monsoon and higher during winter, while the sea-salt component (accumulation and coarse mode) exhibits larger values in monsoon (~32%) and is nearly absent (<2%) in the rest of the year (except of post-monsoon). This high marine-aerosol component over central IGP has been simulated via the iterative OPAC process trying for the best fit between OPAC and measured spectral AODs; similar high (30%) sea-salt component over Kanpur in monsoon was reported by Srivastava and Ramachandran (2013). Organic aerosols, along with BC, are mainly released from biomass burning and urban activities and are accounted for both water soluble and insoluble components (Hess et al., 1998), thus contributing the highest during post-monsoon and winter. During pre-monsoon and monsoon the desert dust (min.tr) presents the highest contribution, especially for the AE days. As far as the AE days is concerned, the highest modifications from the seasonal-mean volume mixing ratios are shown during pre-monsoon and monsoon seasons, when the mineral-transported (dust) component is sharply increased against water soluble and insoluble. Such a result was expected from the CSD curves (Fig. 5), where the coarse-mode fraction increased significantly. The differences are much lower during post-monsoon and winter, mainly detected at a slight higher soot component, a higher dust component in winter and more abundant water-soluble aerosols during post-monsoon on the AE days. This suggests that some of the AEs occurring during winter season may be associated with desert-dust transport (Badarinath et al., 2010), or re-suspension of urban dust due to dry environment. The transported biomass smoke from extensive agriculture burning on the AE days during post-monsoon is the main reason for the increase in water-soluble component. The aerosol volume mixing ratios are in general agreement (at least concerning the seasonal variations) with those reported over Kanpur by Srivastava and Ramachandran (2013). Chemical aerosol characteristics were also analyzed by many over Kanpur (Chinnam et al., 2006; Dey et al., 2008; Dey and Tripathi, 2007, 2008), which are more or less similar to the present findings.

ARF calculations were performed using SBDART model and the results are summarized in Table 3. ARF at TOA is negative (~−12 to −17 Wm^{-2}) in all seasons suggesting cooling effect over central IGP. The attenuation of radiation at surface seems to be large on seasonal basis (−42 to −57 Wm^{-2}), comparable to that found from previous works over Kanpur (Table 3). On the other hand, the atmospheric heating (25–44 Wm^{-2}) contributes to significant warming of the lower-to-middle troposphere. Such a heating, which becomes 70–95% higher during the AE days, causes serious climatic effects over the region and the Himalayan range as discussed by Gautam et al. (2010).

The ARF values are strongly related to higher AODs and modified aerosol properties during the AE days and, therefore, differentiate significantly from the seasonal means. Thus, in winter the seasonal mean ARF values of −49.1, −14.5 and 34.6 Wm^{-2} at surface, TOA and atmosphere change to −88.7, −20.0 and 68.7 Wm^{-2} during the AE days. The enhanced presence of BC in winter, associated with the lower boundary layer height and the absence of precipitation, plays an important role in the large atmospheric forcing values found over IGP (e.g. Ganguly et al., 2005). Furthermore, the atmospheric absorption during major dust storms over Kanpur is strongly depended on dust mineralogy and the Fe mass fraction, while previous studies (Deepshikha et al., 2005; Chinnam et al., 2006) have shown that transported dust over the region is moderately absorbing. Since IGP experiences frequent dust storms during

Table 3
ARF and heating rate values over Kanpur from the present and previous studies. The ARF values during AEs are given in parenthesis. ARF values over whole continental India for further comparison with the present ones can be seen in Dey and Tripathi (2007), Das and Jayaraman (2011, 2012), Sinha et al. (2013a) and many references therein.

Period	Surface (Wm^{-2})	TOA (Wm^{-2})	Atmosphere (Wm^{-2})	Heating Rate ($K\ day^{-1}$)	Reference
Winter (AE)	−49.1 (−88.7)	−14.5 (−20.1)	34.6 (68.7)	1.0 (2.0)	Present study
Pre-monsoon (AE)	−57.0 (−96.6)	−12.8 (−25.6)	44.2 (71.0)	1.2 (2.1)	Present study
Monsoon (AE)	−42.5 (−81.1)	−17.1 (−30.9)	25.4 (50.3)	0.8 (1.6)	Present study
Post-monsoon (AE)	−47.0 (−68.8)	−17.6 (−25.4)	29.5 (43.4)	0.9 (1.5)	Present study
Winter (2006–08)	−33.6	−9.9	23.7	0.44	Ramachandran and Kedia, 2012
Pre-monsoon (2006–08)	−40.7	−4.6	36.2	0.67	Ramachandran and Kedia, 2012
Monsoon (2006–08)	−30.9	−6.3	24.6	0.46	Ramachandran and Kedia, 2012
Post-monsoon (2006–08)	−36.5	−12.0	24.5	0.45	Ramachandran and Kedia, 2012
December 2004	−62	9	71	1.8	Tripathi et al., 2007
May 2004	−26	11	37	~1.02	Chinnam et al., 2006
Dec 2004–Jan 2005	−43	−13	30	0.9	Dey and Tripathi 2007
2001–2005 (annual)	−31.8	−4.1	27.7	0.84	Dey and Tripathi 2008
Apr–June 2006–07	−44	6.8	50.8	–	Gautam et al., 2010

April–June, when the surface albedo also maximizes (Srivastava and Ramachandran, 2013), the dust radiative impact could be significant in view of the climate change over south Asia (Gautam et al., 2011). Srivastava et al. (2012b) examined the ARF and heating rates over Delhi and found much larger anthropogenic contribution during the winter period compared to summer. These findings are in close agreement to the present ones and, in general, to all studies performed over IGP. The difference between surface and TOA ARF suggests the presence of light-absorbing aerosols; thus, the ratio (F) of the surface to the TOA ARF renders as indicator of the aerosol type with $F > 3$ corresponding to strong influence of absorbing aerosols, while values <2 indicate scattering particles (Podgorny et al., 2000). In the current analysis the F values were found to lie between 2.5 (monsoon) and 4.5 (pre-monsoon) for the seasonal means and 2.6 (monsoon) and 4.4 (winter) for the AEs indicating significant contribution of absorbing aerosols and, therefore, atmospheric heating. The heating rate follows the seasonal variation of atmospheric forcing being as high as 1.2 and 2.1 for seasonal mean and AEs, respectively during pre-monsoon. The seasonal-mean values of heating rate are comparable to those found from previous studies over Kanpur, while those during the AE days are almost double. However, the radiative heating rate may be influenced by the vertical distribution and the amount of light-absorbing aerosols above the boundary layer (Moorthy et al., 2009; Lemaitre et al., 2010), while in the present study a vertically homogeneous SSA was used.

3.6. Vertical profiles of aerosol and radiative forcing

ARF depends on the aerosol vertical distribution, especially in the presence of absorbing aerosols (Satheesh et al., 2010). Thus, ARF and heating rates in the atmosphere are estimated on the basis of the measured vertical profiles of the extinction coefficient over Kanpur using the NASA Micro Pulse Lidar Network (MPLNET) data (Welton et al., 2001; Misra et al., 2012) during the period May 2009–September 2010. The NASA MPLNET provides standardized observations of aerosol vertical distribution from a MPL network collocated with AERONET (Welton et al., 2002; Wang et al., 2010). Since the lidar profiles cover only a small part of the study period, the seasonal mean extinction coefficient profiles have been normalized in the vertical using the columnar AODs for the seasonal mean and AE days. Therefore, we achieve mean profiles related to seasonal means and averages of AEs in each season (Fig. 9). The extinction coefficient profiles present extreme values ($>1.0\ km^{-1}$) near the surface during winter and post-monsoon for the AE days, while the seasonal means are comparable to those observed over other urban environments in India (Komppula et al., 2012; Sinha et al., 2013b and references therein). In contrast, in the pre-monsoon and monsoon seasons the extinction coefficient reduces near the surface, while elevated aerosol layers are evident between 2 and 4.5 km. Detailed analysis of the seasonal variation of the MPLNET profiles over Kanpur is given in Misra et al. (2012); so it is beyond the scope of the present work.

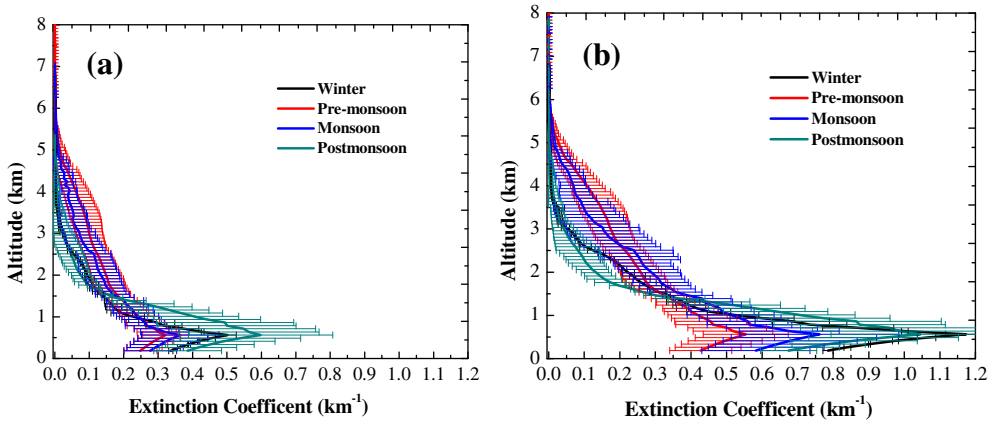

Fig. 9. Normalized profiles of aerosol extinction coefficient for seasonal means (a) and AE days (b). The horizontal bars express one standard deviation. The measured profiles were taken over Kanpur during the period May 2009–September 2010, which have been normalized using the columnar AODs for seasonal means and aerosol episodes during the period 2001–2010.

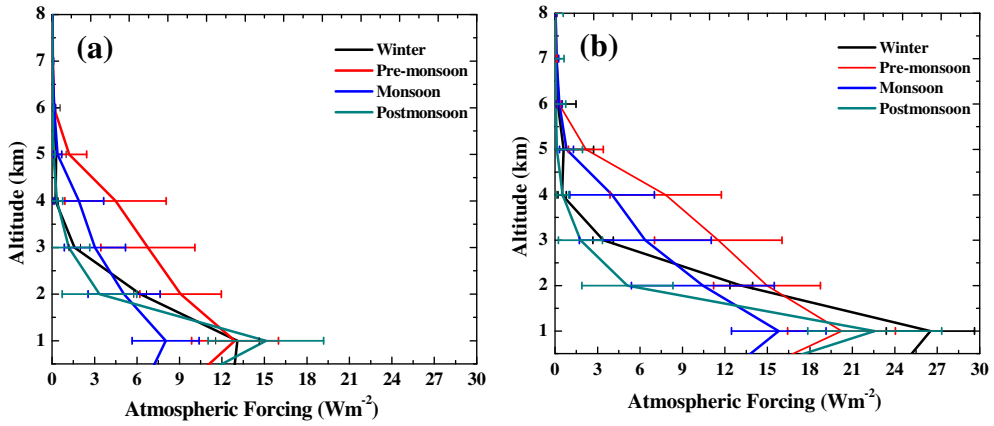

Fig. 10. Vertical profiles of atmospheric forcing estimated using normalized MPLNET lidar profiles of extinction coefficient over Kanpur for seasonal means (a) and AE days (b). The horizontal bars correspond to one standard deviation.

Based on the season-averaged profiles of extinction coefficient, and assuming vertically homogeneous SSA and *g* values (as obtained from Kanpur-AERONET station), the vertical profiles of atmospheric forcing (Fig. 10a, b) and heating rate (Fig. 11a, b) are estimated. As expected, the atmospheric ARF is high (>17 Wm^{-2}) for levels below 2 km during post-monsoon and winter AE days. In contrast, monsoon and mainly pre-monsoon atmospheric forcing for altitudes between 2 and 4.5 km can be considered significant causing serious climate implications on the sea-land temperature gradients, onset, duration and intensity of the monsoon and redistribution of rainfall (e.g. Ramanathan et al., 2005; Gautam et al., 2009b). The vertical profiles of heating rate are proportional to those of atmospheric forcing highlighting the significant contribution of anthropogenic forcing and BC near the surface during post-monsoon and winter, and the influence of dust at elevated layers in late pre-monsoon and monsoon. The vertical profiles of heating rate are much higher than those observed over BoB (Moorthy et al., 2009) and Taiwan (Wang et al., 2010), but the heating rate over Kanpur is slightly lower than that found over Delhi (Srivastava et al., 2012b). Earlier studies have shown that the anthropogenic contribution to radiative forcing and heating rate was 73% over Delhi (Srivastava et al., 2012b) and 65% over Kanpur (Dey and Tripathi, 2008). However, the radiative forcing and heating-rate profiles may be very uncertain, as shown via the standard deviations, since they are very much sensitive on the vertical distribution of aerosols.

Satheesh et al. (2010) carried out a sensitivity analysis examining the role of SSA, surface albedo, aerosol vertical distribution and RH in ARF calculations showing that for highly absorbing aerosols a moderate change in surface albedo can change the TOA forcing even at 50% and the surface forcing at 3%. The sensitivity analysis of the effects of extinction coefficient and SSA profiles on calculated ARF (Moorthy et al., 2009) showed that the realistic SSA profile led to 6% decrease of TOA forcing and 9% increase in surface forcing, resulting to 18% increase in atmospheric heating compared to the case assuming a homogeneous columnar SSA. Similarly, Guan et al. (2010) found that the vertical distribution of aerosol absorption strongly influence the forcing and heating rate profiles, while it has little impact on TOA and surface ARF. This suggests uncertainties in the ARF calculations and heating rate profiles, due to some errors in estimates of the aerosol mixing ratio, surface albedo, vertical aerosol profiles, seasonal mean RH values and assumptions of vertically homogeneous SSA and *g*. The seasonally-averaged lidar profiles used in the present work smooth the heating vertical distribution, which may differentiate in cases when thick elevated aerosol layers of different origin exist. As far as the influence of RH is concerned, sensitivity analysis (Ramachandran and Kedia, 2012) showed that a change in RH as high as 10% (i.e. from 70% to 80%) may affect the computed ARF values at TOA by ~11–57% and those at surface by ~3.1–6.3%, strongly dependent on aerosol type, surface albedo as well as humidity levels. However, in our study the difference between the OPAC-fixed RH values used for the ARF

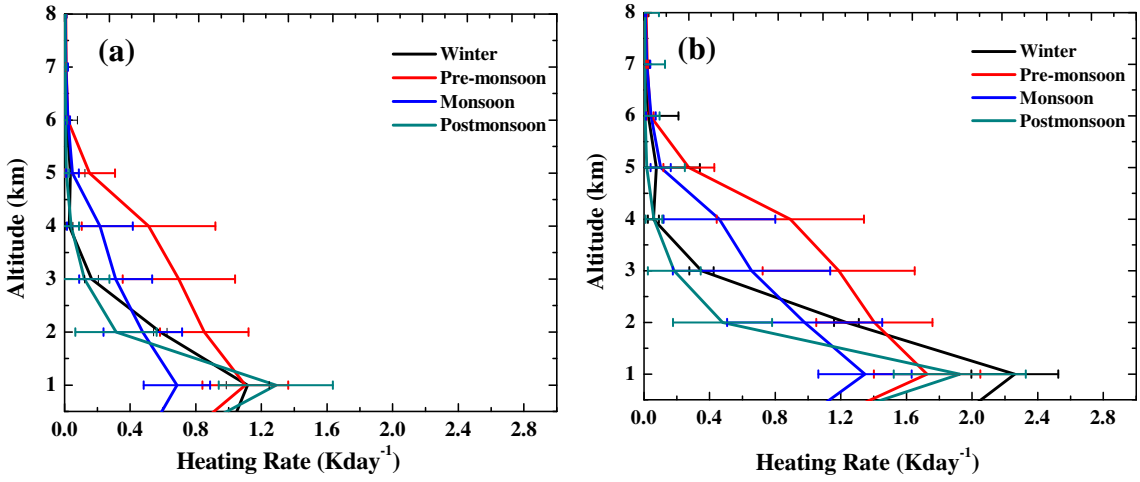

Fig. 11. Same as in Fig. 10, but for the heating rate profiles.

computations and the seasonal-averaged ones measured in Kanpur as much lesser that 10% and, therefore, the ARF values and heating rates are not so significantly affected.

The aerosol optical properties and ARF depend on size, shape and composition of the particles, as well as on RH that determines the growth rate of aerosols. The uncertainty in AERONET spectral AOD is about ±0.02, while that in MODIS-derived surface reflectance ±2%. The uncertainty in the AERONET SSA is within ±0.03 for AOD_{440} >0.5 and increases to 0.05–0.07 for lower AOD (Dubovik and King, 2000), while is in the range of 3–5% for *g* (Andrews et al., 2006), which, however, causes negligible variation in surface, TOA and atmospheric ARF (Mishchenko et al., 1997; McComiskey et al., 2008). Implementing all the above, the overall uncertainty in the calculated ARF values was found to be ~10–15%, similar to that reported by other studies (Dey and Tripathi, 2008; Moorthy et al., 2009). Furthermore, the diurnal variation of ARF and radiative heating rate may be significant (depending on daily variability of aerosols, BC and solar radiation) (Das and Jayaraman, 2011), thus contributing to the uncertainties in the estimated seasonal mean values. In the present work, the daily-mean AERONET retrievals were used in the calculations and the daily-averaged ARF was considered as the half of the estimated value in order to correspond to daytime observations. Taking into account that AERONET retrievals may not cover the whole daytime, this inconsistency provides some uncertainties in the seasonal mean values.

4. Conclusions

Severe aerosol loading over Ganges basin has been recognized as a serious environmental, climatic and health concern and has been the subject of systematic measurements from ground-based instruments and experimental campaigns. This study focuses on examining the occurrence, temporal variation and the influence on aerosol properties and radiative forcing that the aerosol episodes (AEs) have over central Ganges basin. The Kanpur-AERONET data was used covering the period 2001–2010, while the threshold for the determination of AEs was $AOD_{500} = 0.93$, which corresponds to daily AOD_{500} observations above the decadal mean AOD + 1 STD. The analysis revealed the occurrence of 277 AEs out of 2095 daily AOD observations (13.2%), with the majority of them observed during the post-monsoon season, followed by monsoon and winter. It is characteristic that for two periods consisted of 12 days (3–14 November 2008) and 11 days (4–14 June 2003) the AOD_{500} over Kanpur was >0.93. The first case corresponded to a persistent smoke plume from crop-residue burning, while the second was associated with intense dust storms. Furthermore, the aerosol optical properties (AOD, Ångström exponent, columnar size distribution) were analyzed for each season, and separately for the AE days, in order to reveal any modification on them caused by the severe aerosol-laden atmospheres. Synoptically, the analysis showed that except of the seasonality in aerosol optical properties over Kanpur, i.e. dominance of fine-mode aerosols during post-monsoon and winter, and coarse mode during the rest of the year, the AE days were associated with enhanced presence of fine anthropogenic aerosols and/or biomass burning in post-monsoon and winter and coarse dust aerosols in pre-monsoon and monsoon. Similar to observations, OPAC simulations revealed enhanced presence of anthropogenic aerosols and dust in post-monsoon/winter and pre-monsoon/monsoon seasons, respectively, on the AE days compared to the seasonal means. Furthermore, the radiative forcing at surface and TOA was found to be more negative (cooling effect) during the AE days compared to seasonal means, and values as high as −69 to −97 Wm^{-2} at surface and −20 to −30 at TOA were estimated by means of SBDART model. Such forcing values associated with significant atmospheric heating cause serious climate implications over the region, such as modification in the sea-land temperature gradient, influence on the onset, duration and intensity of the monsoon, acceleration in melting of Himalayan glaciers, modification in temperature profile and atmospheric stability and re-distribution of rainfall. Using normalized extinction coefficient profiles obtained from MPLNET over Kanpur, the vertical profiles of atmospheric forcing and heating rate were also estimated. The impact of aerosols on the vertical profiles of solar heating was much larger near the surface in winter and post-monsoon, while in pre-monsoon the heating rate was high (1.2 ± 0.2 Wm^{-2}) between 2 and 4 km.

Acknowledgments

The Kanpur AERONET station was initiated by Drs. R.P. Singh and Brent Holben in 2001. We are thankful to Kanpur PIs (Drs. R.P. Singh, S.N. Tripahi and B.N. Holben) for their efforts in maintaining CIMEL instrument used in the current work. The authors thank E.J. Welton (PI of the Kanpur MPLNET) for his efforts in establishing and maintenance of the lidar network. The current work is supported by the Changing Water Cycle program under MoES, India and NERC UK. SNT acknowledges support from Climate Change Program-Department of Science and Technology Network Programme on "Climate Change Science & Modelling". We also acknowledge the support of IIT Kanpur Flight laboratory for housing Mplnet. The authors are grateful to the anonymous reviewers for their comments/suggestions that have helped us to improve the earlier version of the manuscript.

References

Abish, B., Mohanakumar, K., 2011. Biennial variability in aerosol optical depth associated with QBO modulated tropical tropopause. Atmos. Sci. Lett. 13, 61–66.

Andrews, E., Sheridan, P.J., Fiebig, M., McComiskey, A., Ogren, J.A., Arnott, P., Covert, D., Elleman, R., Gasparini, R., Collins, D., Jonsson, H., Schmid, B., Wang, J., 2006. Comparison of methods for deriving aerosol asymmetry parameter. J. Geophys. Res. 111, D05S04. http://dx.doi.org/10.1029/2004JD005734.

Badarinath, K.V.S., Kharol, S.K., Sharma, A.R., Roy, P.S., 2009a. Fog over Indo-Gangetic Plains—a study using multisatellite data and ground observations. IEEE J. Sel. Top. Appl. Earth Observ. Rem. Sens. 2, 185–195.

Badarinath, K.V.S., Kharol, S.K., Sharma, A.R., 2009b. Long-range transport of aerosols from agriculture crop residue burning in Indo-Gangetic Plains – a study using LIDAR, ground measurements and satellite data. J. Atmos. Sol.-Terr. Phys. 71, 112–120.

Badarinath, K.V.S., Kharol, S.K., Sharma, A.R., Krishna Prasad, V., 2009c. Analysis of aerosol and carbon monoxide characteristics over Arabian Sea during crop residue burning period in the Indo-Gangetic Plains using multi-satellite remote sensing datasets. J. Atmos. Sol.-Terr. Phys. 71, 1267–1276.

Badarinath, K.V.S., Kharol, S.K., Kaskaoutis, D.G., Sharma, A.R., Ramaswamy, V., Kambezidis, H.D., 2010. Long range transport of dust aerosols over Arabian Sea and Indian region – a case study using satellite data and ground-based measurements. Global Planet. Change 72, 164–181.

Badarinath, K.V.S., Kharol, S.K., Kiran Chand, T.R., Madhavi Latha, K., 2011. Characterization of aerosol optical depth, aerosol mass concentration, UV irradiance and black carbon aerosols over Indo-Gangetic plains, India, during fog period. Meteorol. Atmos. Phys. 111, 65–73.

Barman, S.C., Singh, R., Negi, M.P.S., Bhargava, S.K., 2008. Ambient air quality of Lucknow City (India) during use of fireworks on Diwali Festival. Environ. Monit. Assess. 137, 495–504.

Basart, S., Pérez, C., Cuevas, E., Baldasano, J.M., Gobbi, G.P., 2009. Aerosol characterization in Northern Africa, Northeastern Atlantic, Mediterranean Basin and Middle East from direct-sun AERONET observations. Atmos. Chem. Phys. 9, 8265–8282.

Bhawar, R.L., Devara, P.C.S., 2010. Study of successive contrasting monsoons (2001–2002) in terms of aerosol variability over a tropical station Pune, India. Atmos. Chem. Phys. 10, 29–37.

Chinnam, N., Dey, S., Tripathi, S.N., Sharma, M., 2006. Dust events in Kanpur, Northern India: chemical evidence for source and implications to radiative forcing. Geophys. Res. Lett. 33, L08803. http://dx.doi.org/10.1029/2005GL025278.

Das, S.K., Jayaraman, A., 2011. Role of black carbon in aerosol properties and radiative forcing over western India during pre-monsoon period. Atmos. Res. 102, 320–334.

Das, S.K., Jayaraman, A., 2012. Long-range transportation of anthropogenic aerosols over eastern coastal region of India: investigation of sources and impact on regional climate change. Atmos. Res. 118, 68–83.

Das, S.K., Jayaraman, A., Misra, A., 2008. Fog induced variations in aerosol optical and physical properties over the Indo-Gangetic Basin and impact to aerosol radiative forcing. Ann. Geophys. 26, 1345–1354.
Deepshikha, S., Satheesh, S.K., Srinivasan, J., 2005. Regional distribution of absorbing efficiency of dust aerosols over India and adjacent continents inferred using satellite remote sensing. Geophys. Res. Lett. 32, L03811. http://dx.doi.org/10.1029/2004GL022091.
Dey, S., di Girolamo, L., 2010. A climatology of aerosol optical and microphysical properties over the Indian subcontinent from 9 years (2000–2008) of Multi-angle Imaging Spectroradiometer (MISR) data. J. Geophys. Res. 115, D15204. http://dx.doi.org/10.1029/2009JD013395.
Dey, S., Tripathi, S.N., 2007. Estimation of aerosol optical properties and radiative effects in the Ganga Basin, northern India during the winter time. J. Geophys. Res. 112, D03203. http://dx.doi.org/10.1029/2006JD007267.
Dey, S., Tripathi, S.N., 2008. Aerosol direct radiative effects over Kanpur in the Indo-Gangetic basin, northern India, 2008. Long-term (2001–2005) observations and implications to regional climate. J. Geophys. Res. 113, D04212. http://dx.doi.org/10.1029/2007JD009029.
Dey, S., Tripathi, S.N., Singh, R.P., Holben, B.N., 2004. Influence of dust storms on aerosol optical properties over the Indo-Gangetic basin. J. Geophys. Res. 109, D20211. http://dx.doi.org/10.1029/2004JD004924.
Dey, S., Tripathi, S.N., Singh, R.P., Holben, B., 2005. Seasonal variability of the aerosol parameters over Kanpur, an urban site in Indo-Gangetic basin. Adv. Space Res. 36, 778–782.
Dey, S., Tripathi, S.N., Mishra, S.K., 2008. Probable mixing state of aerosols in the Indo-Gangetic Basin, northern India. Geophys. Res. Lett. 35, L03808. http://dx.doi.org/10.1029/2007GL032622.
Dubovik, O., King, M.D., 2000. A flexible inversion algorithm for retrieval of aerosol optical properties from sun and sky radiance measurements. J. Geophys. Res. 105 (D16), 20673–20696.
Dubovik, O., Smirnov, A., Holben, B.N., King, M.D., Kaufman, Y.J., Eck, T.F., Slutsker, I., 2000. Accuracy assessments of aerosol properties retrieved from Aerosol Robotic Network (AERONET) sun and sky radiance measurements. J. Geophys. Res. 105, 9791–9806.
Eck, T.F., Holben, B.N., Reid, J.S., Dubovik, O., Smirnov, A., O'Neill, N.T., Slutsker, I., Kinne, S., 1999. Wavelength dependence of the optical depth of biomass burning, urban, and desert dust aerosols. J. Geophys. Res. 104 (D24), 31333–31349.
Eck, T.F., Holben, B.N., Dubovic, O., Smirnov, A., Goloub, P., Chen, H.B., Chatenet, B., Gomes, L., Zhang, X.Y., Tsay, S.-C., Ji, Q., Giles, D., Slutsker, I., 2005. Columnar aerosol optical properties at AERONET sites in central eastern Asia and aerosol transport to the tropical mid-Pacific. J. Geophys. Res. 110, D06202. http://dx.doi.org/10.1029/2004JD005274.
Eck, T.F., Holben, B.N., Sinyuk, A., Pinker, R.T., Goloub, P., Chen, H., Chatenet, B., Li, Z., Singh, R.P., Tripathi, S.N., Reid, J.S., Giles, D.M., Dubovik, O., O'Neill, N.T., Smirnov, A., Wang, P., Xia, X., 2010. Climatological aspects of the optical properties of fine/coarse mode aerosol mixtures. J. Geophys. Res. 115, D19205. http://dx.doi.org/10.1029/2010JD014002.
Eck, T.F., Holben, B.N., Reid, J.S., Giles, D.M., Rivas, M.A., Singh, R.P., Tripathi, S.N., Bruegge, C.J., Platnick, S., Arnold, G.T., Krotkov, N.A., Carn, S.A., Sinyuk, A., Dubovik, O., Arola, A., Schafer, J.S., Artaxo, P., Smirnov, A., Chen, H., Goloub, P., 2012. Fog- and cloud-induced aerosol modification observed by the Aerosol Robotic Network (AERONET). J. Geophys. Res. 117, D07206. http://dx.doi.org/10.1029/2011JD016839.
El-Askary, H., Gautam, R., Singh, R.P., Kafatos, M., 2006. Dust storms detection over the Indo-Gangetic basin using multi sensor data. Adv. Space Res. 37 (4), 728–733.
Ganguly, D., Gadhavi, H., Jayaraman, A., Rajesh, T.A., Misra, A., 2005. Single scattering albedo of aerosols over the central India: Implications for the regional radiative forcing. Geophys. Res. Lett. 32, L18805. http://dx.doi.org/10.1029/2005GL023903.
Ganguly, D., Jayaraman, A., Rajesh, T.A., Gadhavi, H., 2006. Wintertime aerosol properties during foggy and nonfoggy days over urban center Delhi and their implications for shortwave radiative forcing. J. Geophys. Res. 111, D15217. http://dx.doi.org/10.1029/2005JD007029.
Gautam, R., Hsu, N.C., Kafatos, M., Tsay, S.-C., 2007. Influences of winter haze on fog/low cloud over the Indo-Gangetic plains. J. Geophys. Res. 112, D05207. http://dx.doi.org/10.1029/2005JD007036.
Gautam, R., Liu, Z., Singh, R.P., Hsu, N.C., 2009a. Two contrasting dust-dominant periods over India observed from MODIS and CALIPSO data. Geophys. Res. Lett. 36, L06813. http://dx.doi.org/10.1029/2008GL036967.
Gautam, R., Hsu, N.C., Lau, K.-M., Kafatos, M., 2009b. Aerosol and rainfall variability over the Indian monsoon region: distributions, trends and coupling. Ann. Geophys. 29, 3691–3703.
Gautam, R., Hsu, N.C., Lau, K.-M., 2010. Premonsoon aerosol characterization and radiative effects over the Indo-Gangetic Plains: implications for regional climate warming. J. Geophys. Res. 115, D17208. http://dx.doi.org/10.1029/2010JD013819.
Gautam, R., Hsu, N.C., Tsay, S.C., Lau, K.-M., Holben, B.N., Bell, S., Smirnov, A., Li, C., Hansell, R., Ji, Q., Payra, S., Aryal, D., Kayastha, R., Kim, K.M., 2011. Accumulation of aerosols over the Indo-Gangetic plains and southern slopes of the Himalayas: distribution, properties and radiative effects during the 2009 pre-monsoon Season. Atmos. Chem. Phys. 11, 12841–12863.
Ghude, S.D., Kulkarni, S.H., Kulkarni, P.S., Kanawade, V.P., Fadnavis, S., Pokhrel, S., Jena, C., Beig, G., Bortoli, D., 2011. Anomalous low tropospheric column ozone over Eastern India during the severe drought event of monsoon 2002: a case study. Environ. Sci. Pollut. Res. 18, 1442–1455.
Giles, D.M., Holben, B.N., Tripathi, S.N., Eck, T., Newcomb, W., Slutsker, I., Dickerson, R., Thompson, A., Mattoo, S., Wang, S., Singh, R., Sinyuk, A., Schafer, J., 2011. Aerosol properties over the Indo-Gangetic plain: a 1 mesoscale perspective from the TIGERZ experiment. J. Geophys. Res. 116, D18203. http://dx.doi.org/10.1029/2011JD015809.
Gobbi, G.P., Kaufman, Y.J., Koren, I., Eck, T.F., 2007. Classification of aerosol properties derived from AERONET direct sun data. Atmos. Chem. Phys. 7, 453–458.
Goloub, P., Deuze, J.L., Herman, M., Tanre, D., Chiapello, I., Roger, B., Singh, R.P., 2001. In: Smith, W.L., Timofeyev, Y.M. (Eds.), Aerosol Remote Sensing over Land Using the Spaceborne Polarimeter POLDER. Current Problems in Atmospheric Radiation, pp. 113–116. (Hampton, VA: A Deepak).
Guan, H., Schmid, B., Bucholtz, A., Bergstrom, R., 2010. Sensitivity of short wave radiative flux density, forcing, and heating rate to the aerosol vertical profile. J. Geophys. Res. 115, D06209. http://dx.doi.org/10.1029/2009JD012907.
Guleria, R.P., Kuniyal, J.C., Rawat, P.S., Sharma, N.L., Thakur, H.K., Dhyani, P.P., Singh, M., 2011. The assessment of aerosol optical properties over Mohal in the northwestern Indian Himalayas using satellite and ground-based measurements and an influence of aerosol transport on aerosol radiative forcing. Meteor. Atmos. Phys. 113, 153–169.
Hess, A.M., Koepke, P., Schult, I., 1998. Optical properties of aerosol and clouds: the software package OPAC. Bull. Am. Meteorol. Soc. 79, 831–844.
Holben, B.N., Eck, T.F., Slutsker, I., Tanré, D., Buis, J.P., Setzer, A., Vermote, E., Reagan, J.A., Kaufman, Y.A., 1998. AERONET-a federated instrument network and data achieve for aerosol characterization. Remote Sens. Environ. 66, 1–16.
Jaidevi, J., Gupta, T., Tripathi, S.N., Ujinwal, K., 2009. Assessment of personal exposure to inhalable indoor and outdoor particulate matter for student residents of an academic campus (IIT-Kanpur). Inhalation Toxicol. 21 (14), 1208–1222.
Jaidevi, J., Tripathi, S.N., Gupta, T., Singh, B.N., Gopalakrishnan, V., Dey, S., 2011. Observation-based 3-D view of aerosol radiative properties over Indian Continental Tropical Convergence Zone: implications to regional climate. Tellus 63B, 971–989.
Kar, J., Deeter, M.N., Fishman, J., Liu, Z., Omar, A., Creilson, J.K., Trepte, C.R., Vaughan, M.A., Winker, D.M., 2010. Wintertime pollution over the Eastern Indo-Gangetic Plains as observed from MOPITT, CALIPSO and tropospheric ozone residual data. Atmos. Chem. Phys. 10, 12273–12283.
Kaskaoutis, D.G., Kharol, S.K., Sinha, P.R., Singh, R.P., Badarinath, K.V.S., Mehdi, W., Sharma, M., 2011. Contrasting aerosol trends over South Asia during the last decade based on MODIS observations. Atmos. Measur. Techn. Discuss. 4, 5275–5323.
Kaskaoutis, D.G., Singh, R.P., Gautam, R., Sharma, M., Kosmopoulos, P.G., Tripathi, S.N., 2012a. Variability and trends of aerosol properties over Kanpur, northern India using AERONET data (2001–10). Environ. Res. Lett. 7, 024003.
Kaskaoutis, D.G., Gautam, R., Singh, R.P., Houssos, E.E., Goto, D., Singh, S., Bartzokas, A., Kosmopoulos, P.G., Sharma, M., Hsu, N.C., Holben, B.N., Takemura, T., 2012b. Influence of anomalous dry conditions on aerosols over India: transport, distribution and properties. J. Geophys. Res. 117, D09106. http://dx.doi.org/10.1029/2011JD017314.
Kaul, D.S., Gupta, T., Tripathi, S.N., Tare, V., Collett Jr., J.L., 2011. Secondary organic aerosol: a comparison between foggy and nonfoggy days. Environ. Sci. Tech. 45 (17), 7307–7313.
Kirpa, Ram, Sarin, M.M., Tripathi, S.N., 2010. A 1 year record of carbonaceous aerosols from an urban site in the Indo-Gangetic plain: characterization, sources and temporal variability. J. Geophys. Res. 115, D24313. http://dx.doi.org/10.1029/2010JD014188.
Kirpa, Ram, Sarin, M.M., Tripathi, S.N., 2012. Temporal trends in atmospheric PM2.5, PM10, EC, OC, WSOC and optical properties: impact of biomass burning emissions in the Indo-Gangetic Plain. Environ. Sci. Technol. 46, 686–695.
Komppula, M., Mielonen, T., Arola, A., Korhonen, K., Lihavainen, H., Hyvarinen, A.-P., Baars, H., Engelmann, R., Althausen, D., Ansmann, A., Müller, D., Panwar, T.S., Hooda, R.K., Sharma, V.P., Kerminen, V.-M., Lehtinen, K.E.J., Viisanen, Y., 2012. One year of Raman-lidar measurements in Gual Pahari EUCAARI site close to New Delhi in India: seasonal characteristics of the aerosol vertical structure. Atmos. Chem. Phys. 12, 4513–4524.
Krishna Prasad, V., Ellicott, E., Giglio, L., Badarinath, K.V.S., Vermote, E., Justice, C., Lau, W.K.M., 2012. Vegetation fires in the Himalayan region – aerosol load, black carbon emissions and smoke plume heights. Atmos. Environ. 47, 241–251.
Lemaitre, C., Flamant, C., Cuesta, J., Raut, J.-C., Chazette, P., Formenti, P., Pelon, J., 2010. Radiative heating rates profiles associated with a springtime case of Bodele and Sudan dust transport over West Africa. Atmos. Chem. Phys. 10, 8131–8150.
Liou, K.-N., 2002. An Introduction to Atmospheric Radiation, second ed. International Geophysics Series No. 84 Academic Press.
Lu, Z., Zhang, Q., Streets, D.G., 2011. Sulfur dioxide and primary carbonaceous aerosol emissions in China and India, 1996–2010. Atmos. Chem. Phys. 11, 9839–9864.
Manoj, M.G., Devara, P.C.S., Safai, P.D., Goswami, B.N., 2011. Absorbing aerosols facilitate transition of Indian monsoon breaks to active spells. Clim. Dyn. 37, 2181–2198.
McComiskey, A., Schwartz, S.E., Schmid, B., Guan, H., Lewis, E.R., Richiazzi, P., Ogren, J.A., 2008. Direct aerosol forcing: calculation from observations and sensitivities to inputs. J. Geophys. Res. 113, D09202. http://dx.doi.org/10.1029/2007JD009170.
Menon, S., Hansen, J., Nazarenko, L., Luo, Y., 2002. Climate effects of black carbon aerosols in China and India. Science 297, 2250–2253.

Mishchenko, M.I., Travis, L.D., Kahn, R.A., West, R.A., 1997. Modeling phase functions for dust-like tropospheric aerosols using a shape mixture of randomly oriented polydisperse spheroids. J. Geophys. Res. 102 (16), 831–847.
Mishra, A.K., Shibata, T., 2012. Synergistic analyses of optical and microphysical properties of agricultural cropresidue burning aerosols over the Indo-Gangetic Basin (IGB). Atmos. Environ. 57, 205–218.
Misra, A., Tripathi, S.N., Kaul, D., Welton, E., 2012. Study of MPLNET derived aerosol climatology over Kanpur, India, and validation of CALIPSO Level 2 Version 3 Backscatter and Extinction products. J. Atmos. Oceanic Technol. 29, 1285–1294. http://dx.doi.org/10.1175/JTECH-D-11-00162.1.
Moorthy, K.K., Nair, V.S., Babu, S.S., Satheesh, S.K., 2009. Spatial and vertical heterogeneities in aerosol properties over oceanic regions around India: implications for radiative forcing. Quart. J. Roy. Meteorol. Soc. 135, 2131–2145.
Nair, V.S., Krishna Moorthy, K., Alappattu, D.P., Kunhikrishnan, P.K., George, S., Nair, P.R., Suresh Babu, S., Abish, B., Satheesh, S.K., Tripathi, S.N., Niranjan, K., Madhavan, B.L., Sreekanth, V., Dutt, C.B.S., Badarinath, K.V.S., Reddy, R.R., 2007. Wintertime aerosol characteristics over the Indo-Gangetic Plain (IGP): impacts of local boundary layer processes and long-range transport. J. Geophys. Res. 112, D13205. http://dx.doi.org/10.1029/2006JD008099.
Pathak, B., Kalita, G., Bhuyan, K., Bhuyan, P.K., Moorthy, K.K., 2010. Aerosol temporal characteristics and its impact on shortwave radiative forcing at a location in the northeast of India. J. Geophys. Res. 115, D19204. http://dx.doi.org/10.1029/2009JD013462.
Patidar, V., Tripathi, S.N., Bharti, P., Gupta, T., 2012. First surface measurement of cloud condensation nuclei over Kanpur, IGP: role of long range transport. Aero. Sci. Technol. 46, 973–982.
Podgorny, I.A., Conant, W.C., Ramanathan, V., Satheesh, S.K., 2000. Aerosol modulation of atmospheric and surface solar heating rates over the tropical Indian Ocean. Tellus B 52, 947–958.
Prasad, A.K., Singh, R.P., 2007a. Changes in aerosol parameters during major dust storm events (2001–2005) over the Indo-Gangetic Plains using AERONET and MODIS data. J. Geophys. Res. 112, D09208. http://dx.doi.org/10.1029/2006JD007778.
Prasad, A.K., Singh, R.P., 2007b. Comparison of MISR-MODIS aerosol optical depth over the Indo-Gangetic basin during the winter and summer seasons (2000–2005). Remote. Sens. Environ. 107, 109–119.
Prasad, A.K., Singh, R.P., Kafatos, M., 2006. Influence of coal based thermal power plants on aerosol optical properties in the Indo-Gangetic basin. Geophys. Res. Lett. 33 (5), L05805.
Prasad, A.K., Singh, R.P., Kafatos, M., 2012. Influence of coal-based thermal power plants on the spatial–temporal variability of tropospheric NO_2 column over India. Environ. Monit. Assess. 184, 1891–1907. http://dx.doi.org/10.1007/s10661-011-2087-6.
Ramachandran, S., Kedia, S., 2011. Aerosol radiative effects over an urban location and a remote site in western India: seasonal variability. Atmos. Environ. 45, 7415–7422.
Ramachandran, S., Kedia, S., 2012. Radiative effects of aerosols over Indo-Gangetic plain: environmental (urban vs. rural) and seasonal variations. Environ. Sci. Poll. Res. 19, 2159–2171.
Ramanathan, V., Chung, C., Kim, D., Bettge, T., Buja, L., Kiehl, J.T., Washington, W.M., Fu, Q., Sikka, D.R., Wild, M., 2005. Atmospheric brown clouds: impacts on South Asian climate and hydrological cycle. PNAS 102 (15), 5326–5333. http://dx.doi.org/10.1073/pnas.0500656102.
Reddy, M.S., Venkataraman, C., 2002. Inventory of aerosol and sulphur dioxide emission from India: II-Biomass combustion. Atmos. Environ. 36, 699–712.
Reid, J.S., Eck, T.F., Christopher, S.A., Hobbs, P.V., Holben, B.N., 1999. Use of the Ångström exponent to estimate the variability of optical and physical properties of aging smoke particles in Brazil. J. Geophys. Res. 104 (D22), 27473–27489.
Ricchiazzi, P., Yang, S., Gautier, C., Sowle, D., 1998. SBDART: a research and teaching software tool for plane-parallel radiative transfer in the Earth's atmosphere. Bull. Amer. Meteorol. Soc. 79, 2101–2114.
Satheesh, S.K., Vinoj, V., Moorthy, K.K., 2010. Radiative effects of aerosols at an urban location in southern India: observations versus model. Atmos. Environ. 44, 5295–5304.
Schuster, G.L., Dubovik, O., Holben, B.N., 2006. Ångström exponent and bimodal aerosol size distributions. J. Geophys. Res. 111, D07207. http://dx.doi.org/10.1029/2005JD006328.
Sharma, A.R., Kharol, S.K., Badarinath, K.V.S., Singh, D., 2010. Impact of agriculture crop residue burning on atmospheric aerosol loading – a study over Punjab State, India. Ann. Geophys. 28, 367–379.
Singh, R.P., 2010. Interactive comment on "Inferring absorbing organic carbon content from AERONET data" by A. Arola et al. Interactive Comment on Atmos. Chem. Phys. Discuss. 10, 18365.
Singh, R.P., Dey, S., Tripathi, S.N., Tare, V., Holben, B.N., 2004. Variability of aerosol parameters over Kanpur, northern India. J. Geophys. Res. 109, D23206. http://dx.doi.org/10.1029/2004JD004966.
Singh, S., Soni, K., Bano, T., Tanwar, R.S., Nath, S., Arya, B.C., 2010. Clear-sky direct aerosol radiative forcing variations over mega-city Delhi. Ann. Geophys. 28, 1157–1166.
Sinha, P.R., Dumka, U.C., Manchanda, R.K., Kaskaoutis, D.G., Sreenivasan, S., Krishna Moorthy, K., Suresh Babu, S., 2013a. Contrasting aerosol characteristics and radiative forcing over Hyderabad, India due to seasonal meso-scale and synoptic scale processes. Q. J. R. Meteorol. Soc. 139, 434–450. http://dx.doi.org/10.1002/qj.1963.
Sinha, P.R., Kaskaoutis, D.G., Manchanda, R.K., Sreenivasan, S., 2012. Characteristics of aerosols over Hyderabad, in Southern Peninsular India with the use of different techniques. Ann. Geophys. 30, 1393–1410.
Sinha, P.R., Manchanda, R.K., Kaskaoutis, D.G., Kumar, Y.B., Sreenivasan, S., 2013b. Seasonal variation of surface and vertical profile of aerosol properties over a tropical urban station Hyderabad, India. J. Geophys. Res. 118, 749–768. http://dx.doi.org/10.1029/2012JD018039.
Smirnov, A., Holben, B.N., Eck, T.F., Dubovik, O., Slutsker, I., 2000. Cloud screening and quality control algorithms for the AERONET data base. Remote Sens. Environ. 73, 337–349.
Srivastava, R., Ramachandran, S., 2013. The mixing state of aerosols over the Indo-Gangetic Plain and its impact on radiative forcing. Q. J. R. Meteorol. Soc. 139, 137–151.
Srivastava, A.K., Singh, S., Tiwari, S., Kanawade, V.P., Bisht, D.S., 2012a. Variation between near-surface and columnar aerosol characteristics during the winter and summer at Delhi in the Indo-Gangetic Basin. J. Atmos. Sol.-Terr. Phys. 77, 57–66.
Srivastava, A.K., Singh, S., Tiwari, S., Bisht, D.S., 2012b. Contribution of anthropogenic aerosols in direct radiative forcing and atmospheric heating rate over Delhi in the Indo-Gangetic Basin. Environ. Sci. Pollut. Res. 19, 1144–1158.
Srivastava, A.K., Tiwari, S., Devara, P.C.S., Bisht, D.S., Srivastava, M.K., Tripathi, S.N., Goloub, P., Holben, B.N., 2012c. Pre-monsoon aerosol characteristics over the Indo-Gangetic Basin: implications to climatic impact. Ann. Geophys. 29, 789–804.
Srivastava, A.K., Tripathi, S.N., Dey, S., Kanawade, V.P., Tiwari, S., 2012d. Inferring aerosol types over the Indo-Gangetic Basin from ground based sun photometer measurements. Atmos. Res. 109, 64–75.
Streets, D.G., Bond, T.C., Carmichael, G.R., Fernandes, S.D., Fu, Q., He, D., Klimont, Z., Nelson, S.M., Tsai, N.Y., Wang, M.Q., Woo, J.-H., Yarber, K.F., 2003. An inventory of gaseous and primary aerosol emissions in Asia in the year 2000. J. Geophys. Res. 108 (D21), 8809. http://dx.doi.org/10.1029/2002JD003093.
Tripathi, S.N., Srivastva, A.K., Dey, S., Satheesh, S.K., Krishnamoorthy, K., 2007. The vertical profile of atmospheric heating rate of black carbon aerosols at Kanpur in northern India. Atmos. Environ. 41, 6909–6915.
Venkataraman, C., Habib, G., Kadamba, D., Shrivastava, M., Leon, J.-F., Crouzille, B., Boucher, O., Streets, D.G., 2006. Emissions from open biomass burning in India: integrating the inventory approach with high-resolution moderate resolution imaging spectroradiometer (MODIS) active-fire and land cover data. Global Biogeochem. Cyc. 20, GB2013. http://dx.doi.org/10.1029/2005GB002547.
Verma, S., Venkataraman, C., Boucher, O., 2012. Attribution of aerosol radiative forcing over India during the winter monsoon to emissions from source categories and geographical regions. Atmos. Environ. 45, 4398–4407.
Wang, S.-H., Lin, N.-H., Chou, M.-D., Tsay, S.-C., Welton, E.J., Hsu, N.C., Giles, D.M., Liu, G.-R., Holben, B.N., 2010. Profiling transboundary aerosols over Taiwan and assessing their radiative effects. J. Geophys. Res. 115, D00K31. http://dx.doi.org/10.1029/2009JD013798.
Wang, S., Fang, L., Gu, X., Yua, T., Gao, J., 2011. Comparison of aerosol optical properties from Beijing and Kanpur. Atmos. Environ. 45, 7406–7414.
Welton, E.J., Campbell, J.R., Spinhirne, J.D., Scott, V.S., 2001. Global monitoring of clouds and aerosols using a network of micro-pulse lidar systems. Proc. SPIE Int. Soc. Opt. Eng. 4153, 151–158.
Welton, E.J., Voss, K.J., Quinn, P.K., Flatau, P.J., Markowicz, K., Campbell, J.R., Spinhirne, J.D., Gordon, H.R., Johnson, J.E., 2002. Measurements of aerosol vertical profiles and optical properties during INDOEX 1999 using micropulse lidars. J. Geophys. Res. 107 (D19), 8019. http://dx.doi.org/10.1029/2000JD000038.
Yoon, J., von Hoyningen-Huene, W., Kokhanovsky, A.A., Vountas, M., Burrows, J.P., 2011. Trend analysis of the aerosol optical thickness and Ångström exponent derived from the global AERONET spectral observations. Atmos. Meas. Tech. Discuss. 4, 5325–5388.